Phonons in disordered alloys: Comparison between augmented-space-based approximations for configuration averaging to integration from first principles

Aftab Alam
S.N. Bose National Center for Basic Sciences, JD Block, Sector III, Salt Lake City, Kolkata 700 098, India

Subhradip Ghosh
Department of Physics, Indian Institute of Technology, Guwahati, Assam, India

Abhijit Mookerjee*
Department of Physics, Indian Institute of Technology, Kanpur, Uttar Pradesh, India
(Received 10 October 2006; revised manuscript received 18 December 2006; published 23 April 2007)

A first principles density functional based linear response theory (the so-called density functional perturbation theory [Baroni *et al.*, Rev. Mod. Phys. **73**, 515 (2001)] has been combined separately with two recently developed formalisms for a systematic study of the lattice dynamics in disordered binary alloys. The two formalisms are the augmented space recursion (ASR) [Alam *et al.*, Phys. Rev. B **69**, 024205 (2004)] and the itinerant coherent potential approximation (ICPA) [Ghosh *et al.*, Phys Rev. B **66**, 214206 (2002)]. The two different theories (DFPT-ASR and DFPT-ICPA) systematically provides a hierarchy of improvements upon the earlier single site based theories (like CPA, etc.) and includes nonlocal correlations in the disorder configurations. The formalisms explicitly take into account fluctuations in masses, force constants and scattering lengths. The combination of DFPT with these formulations helps in understanding the actual interplay of force constants in alloys. We illustrate the methods by applying to a fcc $Fe_{50}Pd_{50}$ alloy.

DOI: 10.1103/PhysRevB.75.134202 PACS number(s): 36.40.Cg, 75.50.Pp

I. INTRODUCTION

The last 30 years have seen numerous attempts at setting up a quantitatively accurate theory of phonons in disordered alloys. One of the earliest successful approximations was the coherent potential approximation[4] (CPA). This approximation was a considerable improvement on the existing theories and, in examples of homogeneous disorder, was shown to yield configuration averaged Green functions which maintained lattice translational symmetry and the herglotz analytical properties[5] essential for physical interpretation.[6] Despite its success, particularly in the electronic problem, the CPA was a single-site, mean-field approximation and could deal with only diagonal (or mass, in the case of phonons) disorder. The phonon problem is specifically difficult because, in it, diagonal and off-diagonal disorders are impossible to separate. Moreover, the sum rule satisfied between the diagonal and off-diagonal parts of the force-constants leads to environmental disorder. That is, a configuration fluctuation at a site affects the diagonal part of the dynamical matrix at its neighbors. Consequently, we do not expect the CPA to give an adequate description of the phonon problem. This was discussed in several papers,[7–12] which indicated large discrepancies between the CPA predictions and experimental results. In the electron problem too, whenever there was off-diagonal disorder, as in the case of alloys with large size difference between its constituents leading to local lattice distortions[13] or environmental disorder as in the case of alloys with short-range order,[14,15] the CPA was found to be inadequate.

The hunt for adequate extensions of the CPA was quite rigorous during the 1970s and 1980s.[16–20] Most of these generalizations were valid for very special types of off-diagonal disorder, which were mostly unphysical, or violated translational symmetry and herglotz properties. Eventually, three approaches emerged as the most successful. Two of them were based on the augmented-space theorem of Mookerjee:[21] the itinerant coherent-potential approximation (ICPA) of Ghosh *et al.*[3] and the augmented-space recursion (ASR) of Saha *et al.*[22] and Alam *et al.*[2] The former was an extension of the ideas of Mills and Ratanavaraksa[23] and Kaplan *et al.*[24] and the latter combined the augmented-space technique with the recursion method of Haydock *et al.*[25] The third was a very different and rather striking approach developed by Rowlands *et al.*[26] and Biava *et al.*[27] (the nonlocal CPA or NL-CPA) using the idea of *coarse graining* in reciprocal space originally proposed by Jarell and Krishnamurthy.[28]

More importantly a first principles *ab initio* theory of phonons in disordered alloys is still lacking. Such a theory is needed in order to gain a microscopic understanding of the interplay of force constants in the complex phenomenon of phonon excitations. Our aim in this paper is twofold: First, we shall discuss the similarities and differences between the two methods (ICPA and ASR) based on the augmented-space theorem. We shall apply both the techniques to identical models of an alloy system, FePd, and discuss the comparison between their results. Second, we shall estimate the dynamical matrices from a first-principles approach to the parent ordered alloys and compare the ICPA and ASR results with experiment. We shall argue that first-principles estimates of the dynamical matrices on ordered versions do not yield quantitatively accurate results (in comparison with experiment) for the disordered alloys. We shall propose that we need to go beyond and estimate the dynamical matrices from a model of embedded atoms in a fully disordered background.

The outline of this paper is as follows. In Sec. II, we shall discuss in brief what the augmented-space theorem is and its application to the problem of phonon excitations in disordered alloys. In Sec. III), we shall briefly describe the salient features of itinerant coherent potential approximation (ICPA) and the augmented-space recursion (ASR). Sec. IV shall be devoted for the details of first-principles calculation of force constants in alloys. The numerical results shall be discussed in Sec. V. Finally conclusions are drawn in Sec. VI.

II. THE AUGMENTED-SPACE THEOREM

The augmented-space theorem has been discussed in great detail elsewhere.[29] In this section we shall introduce only those salient features which will be required by us to understand the mathematics and notations in our subsequent discussions.

For a homogeneously disordered binary alloy the Green function may be written as

$$\langle\langle \mathbf{G}(\mathbf{k},\omega^2)\rangle\rangle = \frac{1}{N}\sum_{R,R'} \exp\{i\mathbf{k}\cdot(R-R')\} \times \langle\langle\langle R|(\mathbf{m}\omega^2-\mathbf{\Phi})^{-1}|R'\rangle\rangle\rangle,$$

$$\mathbf{m} = \{\mathbf{m}^A n_R + \mathbf{m}^B(1-n_R)\}\delta_{RR'},$$

$$\mathbf{\Phi} = \mathbf{\Phi}^{AA}_{R-R'} n_R n_{R'} + \mathbf{\Phi}^{BB}_{R-R'}(1-n_R)(1-n_{R'}) + \mathbf{\Phi}^{AB}_{R-R'}\{n_R(1-n_{R'})+(1-n_R)n_{R'}\}. \quad (1)$$

Here, R,R' refer to lattice positions, $\langle\langle\ \rangle\rangle$ refers to configuration averaging over random variables in the problem. We should note here that the Fourier transform in the first equation may be taken *only* after the configuration averaging is carried out. The mass and force-constant matrices are matrices in the mode space and for systems with one atom per unit cell they are 3×3. $\{n_R\}$ are the random site-occupation variables which take values 1 and 0 depending upon whether the site labelled by R is occupied by A- or B-type of atom. The atom sitting at R can either be of type $A(n_R=1)$ with probability x or $B(n_R=0)$ with probability y. The augmented-space formalism (ASF) now introduces the space of configurations of the set of binary random variables $\{n_R\}$: Ψ.

In the absence of short-ranged order, each random variable n_R has associated with it an operator $\mathbf{M}_R$ whose spectral density is its probability density,

$$p(n_R) = x\delta(n_R-1) + y\delta(n_R) = -\frac{1}{\pi}\lim_{\delta\to 0}\mathrm{Im}\langle\uparrow_R|((n_R+i\delta)\mathbf{I}-\mathbf{M}_R)^{-1}|\uparrow_R\rangle, \quad (2)$$

where x,y are concentrations of the components A and B, $\mathbf{M}_R$ is an operator whose eigenvalues 1, 0 correspond to the observed values of n_R and whose corresponding eigenvectors $\{|1_R\rangle,|0_R\rangle\}$ span a configuration space ψ_R of rank 2. We may change the basis to $\{|\uparrow_R\rangle,|\downarrow_R\rangle\}$,

$$|\uparrow_R\rangle = \{\sqrt{x}|1_R\rangle + \sqrt{y}|0_R\rangle\},$$

$$|\downarrow_R\rangle = \{\sqrt{y}|1_R\rangle - \sqrt{x}|0_R\rangle\},$$

and in the new basis the operator $\mathbf{M}_R$ corresponding to n_R is

$$\mathbf{M}_R = x\mathcal{P}^{\uparrow}_R + y\mathcal{P}^{\downarrow}_R + \sqrt{xy}\mathcal{T}^{\uparrow\downarrow}_R,$$

where $\mathcal{P}^{\uparrow}_R=|\uparrow_R\rangle\langle\uparrow_R|$, $\mathcal{P}^{\downarrow}_R=|\downarrow_R\rangle\langle\downarrow_R|$ and $\mathcal{T}^{\uparrow\downarrow}_R=|\uparrow_R\rangle\langle\downarrow_R| + |\downarrow_R\rangle\langle\uparrow_R|$ are the projection and transfer operators in the configuration space ψ_R spanned by the two basis vectors.

The full configuration space $\mathbf{\Psi}=\Pi^{\otimes}_R\psi_R$ is then spanned by vectors of the form $|\uparrow\uparrow\downarrow\uparrow\downarrow\cdots\rangle$. These configurations may be labelled by the sequence of sites $\{\mathcal{C}\}$ at which we have a $\downarrow$. For example, for the state just quoted $\{\mathcal{C}\}=|\{3,5,\ldots\}\rangle$. This sequence is called the *cardinality sequence*. If we define the configuration $|\uparrow\uparrow\cdots\uparrow\cdots\rangle$ as the *reference* configuration, then the *cardinality sequence* of the *reference* configuration is the null sequence $\{\varnothing\}$.

In the full augmented-space the operator corresponding to n_R is

$$\hat{\mathbf{M}}_R = \mathcal{I}\otimes\cdots\otimes\mathbf{M}_R\otimes\cdots\otimes\mathcal{I}\otimes\cdots\in\mathbf{\Psi}.$$

The augmented-space theorem[21] then yields

$$\langle\langle \mathbf{G}(\mathbf{k},\omega^2)\rangle\rangle = \langle\mathbf{k}\otimes\{\varnothing\}|(\hat{\mathbf{m}}\omega^2-\hat{\mathbf{\Phi}})^{-1}|\mathbf{k}\otimes\{\varnothing\}\rangle, \quad (3)$$

where the augmented $\mathbf{k}$-space basis $|\mathbf{k}\otimes\{\varnothing\}\rangle$ has the form

$$(1/\sqrt{N})\sum_R \exp(-i\mathbf{k}\cdot R)|R\otimes\{\varnothing\}\rangle.$$

The augmented-space operators $\hat{\mathbf{m}}$ and $\hat{\mathbf{\Phi}}$ are constructed from the original random operators by replacing each random variable n_R by the operators $\hat{\mathbf{M}}_R$. It is an operator in the augmented space $\mathbf{\Xi}=\mathcal{H}\otimes\mathbf{\Psi}$. The theorem maps a disordered operator described in a Hilbert space $\mathcal{H}$ onto an ordered one in an enlarged space $\mathbf{\Xi}$, where this space is constructed as the outer product of the space $\mathcal{H}$ and configuration space $\mathbf{\Psi}$ of the random variables. The configuration space $\mathbf{\Psi}$ is of rank 2^N if there are N sites in the system. Another way of looking at the augmented-space operators is to note that they are *collection* of all possible operators for all possible configurations of the system.

The augmented-space operators may be written as:[2]

$$\hat{\mathbf{m}} = \langle\langle\mathbf{m}\rangle\rangle\hat{\mathbf{I}} + (\mathbf{m}_A-\mathbf{m}_B)\sum_R \mathcal{P}_R\otimes[(y-x)\mathcal{P}^{\downarrow}_R + \sqrt{xy}\mathcal{T}^{\uparrow\downarrow}_R],$$

$$\hat{\Phi}_{\mathrm{off}} = \sum_R\sum_{R\neq R'}\mathcal{T}_{RR'}\otimes\{\langle\langle\mathbf{\Phi}_{RR'}\rangle\rangle\mathcal{I} + \mathbf{\Phi}^{(1)}_{RR'}[(y-x)(\mathcal{P}^{\downarrow}_R+\mathcal{P}^{\downarrow}_{R'}) + \sqrt{xy}(\mathcal{T}^{\uparrow\downarrow}_R+\mathcal{T}^{\uparrow\downarrow}_{R'})] + \mathbf{\Phi}^{(2)}_{RR'}[\sqrt{xy}(y-x)(\mathcal{P}^{\downarrow}_R\otimes\mathcal{T}^{\uparrow\downarrow}_{R'}+\mathcal{P}^{\downarrow}_{R'}\otimes\mathcal{T}^{\uparrow\downarrow}_R) + (y-x)^2\mathcal{P}^{\downarrow}_R\otimes\mathcal{P}^{\downarrow}_{R'} + xy\mathcal{T}^{\uparrow\downarrow}_R\otimes\mathcal{T}^{\uparrow\downarrow}_{R'}]\},$$

$$\hat{\Phi}_{\text{dia}} = \sum_R \mathcal{P}_R \otimes \Bigg(- \langle\langle \mathbf{\Phi}_{RR} \rangle\rangle \mathcal{I} - \sum_{R' \neq R} \mathbf{\Phi}^{(1)}_{RR'} [(y-x)\mathcal{P}^{\downarrow}_R + \sqrt{xy}\mathcal{T}^{\uparrow\downarrow}_R] - \sum_{R' \neq R} \mathbf{\Phi}^{(1)}_{RR'} [(y-x)\mathcal{P}^{\downarrow}_{R'} + \sqrt{xy}\mathcal{T}^{\uparrow\downarrow}_{R'}] - \sum_{R' \neq R} \mathbf{\Phi}^{(2)}_{RR'} [\sqrt{xy}(y-x)(\mathcal{P}^{\downarrow}_R \otimes \mathcal{T}^{\uparrow\downarrow}_{R'} + \mathcal{P}^{\downarrow}_{R'} \otimes \mathcal{T}^{\uparrow\downarrow}_R) + (y-x)^2 \mathcal{P}^{\downarrow}_R \otimes \mathcal{P}^{\downarrow}_{R'} + xy \mathcal{T}^{\uparrow\downarrow}_R \otimes \mathcal{T}^{\uparrow\downarrow}_{R'}] \Bigg),$$

$$\hat{\Phi} = \hat{\Phi}_{\text{dia}} + \hat{\Phi}_{\text{off}}, \tag{4}$$

where

$$\mathbf{\Phi}^{(1)}_{RR'} = x\mathbf{\Phi}^{AA}_{RR'} - y\mathbf{\Phi}^{BB}_{RR'} + (y-x)\mathbf{\Phi}^{AB}_{RR'},$$

$$\mathbf{\Phi}^{(2)}_{RR'} = \mathbf{\Phi}^{AA}_{RR'} + \mathbf{\Phi}^{BB}_{RR'} - 2\mathbf{\Phi}^{AB}_{RR'}.$$

The sum rule which connects the diagonal and off-diagonal parts of the force-constant matrices has been incorporated into the formulation.

III. THE ITINERANT COHERENT POTENTIAL APPROXIMATION AND AUGMENTED-SPACE RECURSION

The augmented-space theorem described in the preceding section is an *exact* statement. It is a clever book-keeping technique to include the effects of disorder fluctuations in the model of phonons in our random alloy. However, it is not an algorithm for the approximate calculations of spectral and other physical properties of phonons in disordered alloys. For that we must turn to either mean-field approximations like the CPA and ICPA or alternatively to the ASR. The coherent potential like mean-field approximations begin with a *partition* of the augmented space into a part which is spanned by the *reference* or *null cardinality* state $|\{\varnothing\}\rangle$ which we shall call the *average* configuration state and the remaining part $\mathbf{\Psi} - |\{\varnothing\}\rangle\langle\{\varnothing\}|$ spanned by *fluctuation* states: $\{|\{\mathcal{C}\}\rangle\}$. With this partition, any operator can be written in a block representation,

$$\mathbf{A} = \begin{pmatrix} \mathbf{A}_1 & \mathbf{A}' \\ \mathbf{A}'^{\dagger} & \mathbf{A}_2 \end{pmatrix}.$$

The partition or downfolding theorem then allows us to invert this operator in the subspace spanned by the *average* configurations alone. By the augmented-space theorem this is the configuration average. If we define the operator $\mathbf{K}$ as $(\mathbf{m}\omega^2 - \mathbf{\Phi})$, then using the above partition: $\mathbf{K}_1 = (\langle\langle \mathbf{m} \rangle\rangle \omega^2 - \langle\langle \mathbf{\Phi} \rangle\rangle)$. The downfolding theorem and augmented-space theorem together give us

$$\langle\langle \mathbf{G}(\omega^2) \rangle\rangle = (\mathbf{K}_1 - \mathbf{K}'^{\dagger}\mathbf{F}\mathbf{K}')^{-P_1} = (\mathbf{G}^{-1}_{VCA}(\omega^2) - \mathbf{\Sigma}(\omega^2))^{-P_1},$$

$$\mathbf{F} = \mathbf{K}_2^{-P_2} \text{ is the itinerator,} \tag{5}$$

$$\mathbf{\Sigma} = \mathbf{K}'^{\dagger}\mathbf{F}\mathbf{K}' \text{ is the self-energy.} \tag{6}$$

Here $\mathbf{A}^{-P_1}$ and $\mathbf{A}^{-P_2}$ refer to the inverses of the operator $\mathbf{A}$ in the subspaces labelled by 1 and 2. This is exactly the partitioning idea introduced by Srivastava *et al.*[30] Ghosh *et al.*[3] next confined themselves to *single fluctuation* states of the type $|\{R\}\rangle$ and went ahead to self-consistently evaluate the self-energy in this approximation. Adopting their notation $\langle\{R\}|\mathbf{A}|\{R'\}\rangle = A^{(R)(R')}$, they used translational symmetry in augmented space[31] and approximated the self-energy and *itinerator* $\mathbf{F}$ within the single fluctuation states,

$$\mathbf{\Sigma} = \sum_{RR'} \mathbf{K}'^{\dagger(R)} \mathbf{F}^{(R)(R')} \mathbf{K}'^{(R')}, \tag{7}$$

$$\mathbf{F}^{(R)(R')} = \mathbf{G}^{(R)} \Bigg(\delta_{RR'} + \sum_{R''} \mathbf{V}^{(R)(R'')} F^{(R'')(R')} \Bigg). \tag{8}$$

In going from Eq. (5)–(7) all contributions to the self-energy of configuration states with more than one fluctuation in more than one site have been neglected. Similarly in going from Eq. (6)–(8), matrix elements of the itinerator $\mathbf{F}$ between configuration states with more than one fluctuation present at a time, which corresponds to coherent scattering from more than one site have been neglected and such states do not contribute to $\mathbf{F}$ and hence to the self-energy $\mathbf{\Sigma}$ within this approximation. The second equation is a Dyson equation within the subspace spanned by only single fluctuation states. Self-consistency is achieved through

$$\mathbf{G}^{(R)} = (\mathbf{G}^{-1}_{VCA} - \mathbf{\Sigma}^{(R)})^{-1},$$

$$\mathbf{\Sigma}^{(R)} = \sum_{R'R'' \neq R} \mathbf{K}'^{(R')} \mathbf{F}^{(R')(R'')} \mathbf{K}'^{(R'')}.$$

The above argument shows that unlike the usual CPA where only a single fluctuation at a site is considered, multiple fluctuations coming from multiple scattering is present in the itinerator $\mathbf{F}$ and therefore contribute to the self-energy $\mathbf{\Sigma}$. However, the approximation described above means that correlated fluctuations between more than one site are present in neither the itinerator nor the self-energy. This is the main approximation involved in the ICPA.

We note that the ICPA is a self-consistent mean-field approximation for the self-energy which relates the configuration averaged Green function to the virtual crystal one. It is an approximation which maintains both the translational symmetry of the configuration average and its herglotz analytic properties. The ASR is an alternative technique for doing the same thing, namely obtaining an approximation to the self-energy maintaining the necessary properties of the exact case.

The recursion method addresses inversions of infinite matrices.[32] The average Green function in the augmented-space formalism can be written as[2]

$$\langle\langle \mathbf{G} \rangle\rangle = \{1|(\omega'^2\hat{\mathbf{I}} - \tilde{\mathbf{K}})^{-1}|1\}.$$

Here

$$\omega' = \mu^{1/2}\omega,$$

$$\hat{\mathbf{K}} = (\hat{\mathbf{m}^{1/2}}\mu^{1/2})\hat{\mathbf{\Phi}}(\hat{\mathbf{m}^{1/2}}\mu^{1/2}),$$

$$|1\} = (\mu_1^{-1/2}\mu^{1/2})|\{\varnothing\}\rangle + (\mu_2^{-1/2}\mu^{1/2})|\{R\}\rangle,$$

where $\mu^{1/2} = \ll m^{-1} \gg^{-1/2}$, $\mu_1^{-1/2} = \ll m^{-1/2} \gg$ and $\mu_2^{-1/2} = \sqrt{xy}(m_A^{-1/2} - m_B^{-1/2})$.

Once a sparse representation of an operator in a Hilbert space, $\hat{\mathbf{K}}$, is known in a countable basis, the recursion method obtains an alternative basis in which the operator becomes tridiagonal. This basis and the representations of the operator in it are found recursively through a three-term recurrence relation

$$|u_{n+1}\} = \hat{\mathbf{K}}|u_n\} - \alpha_n(\mathbf{k})|u_n\} - \beta_n^2(\mathbf{k})|u_{n-1}\} \tag{9}$$

with the initial choice $|u_1\} = |\mathbf{k} \otimes \{1\}\rangle$ or $\beta_1^2 = 1$. The recursion coefficients α_n and β_n are real and are obtained by imposing the orthonormalizability condition of the new basis set as

$$\alpha_n(\mathbf{k}) = \frac{\{u_n|\hat{\mathbf{K}}|u_n\}}{\{u_n|u_n\}}, \quad \beta_{n+1}^2(\mathbf{k}) = \frac{\{u_n|\hat{\mathbf{K}}|u_{n+1}\}}{\{u_n|u_n\}}$$

and also $\{u_m|u_n\} = 0$ for $m \neq n, n \pm 1$.

Now, we use the augmented-space theorem and repeated applications of the downfolding theorem on the tridiagonal representation gives

$$\langle\langle \mathbf{G}(\mathbf{k},\omega'^2)\rangle\rangle = \cfrac{1}{\omega'^2 - \alpha_1(\mathbf{k}) - \cfrac{\beta_2^2(\mathbf{k})}{\omega'^2 - \alpha_2(\mathbf{k}) - \cfrac{\beta_3^2(\mathbf{k})}{\ddots \cfrac{}{\omega'^2 - \alpha_N(\mathbf{k}) - \mathbf{\Gamma}(\mathbf{k},\omega'^2)}}}} = \frac{1}{\omega'^2 - \alpha_1(\mathbf{k}) - \Sigma'(\mathbf{k},\omega'^2)}. \tag{10}$$

From the definition of the self-energy given earlier, it has been argued by us in an earlier paper that the disorder scattering induced lifetimes come entirely from the imaginary part of $\Sigma'(\mathbf{k},\omega'^2)$. Here $\mathbf{\Gamma}(\mathbf{k},\omega'^2)$ is the asymptotic part of the continued fraction. The *approximation* involved has to do with the termination of this continued fraction. The coefficients are calculated exactly up to a finite number of steps $\{\alpha_n, \beta_n\}$ for $n < N$ and the asymptotic part of the continued fraction is obtained from the initial set of coefficients using the idea of Beer and Pettifor terminator.[33] With this terminator, the approximate Green function maintains the herglotz properties of the exact result. Haydock and co-workers[25] have carried out extensive studies of the errors involved and precise estimates are available in the literature. Haydock[25] has shown that if we carry out recursion exactly up to N steps, the resulting continued fraction maintains the first $2N$ moments of the exact result.

Both the ICPA and the ASR involve approximations of the self-energy. We have already discussed that in the ICPA contributions of configurations involving correlated fluctuations in more than one site to the self-energy are ignored in the present case but it is capable of incorporating them. If we use the form of Eq. (4) in the recursion equations (9), it is immediately obvious that in the ASR, contributions of such correlated fluctuation states to the self-energy are present. We had earlier shown that such contributions occur first at β_4^2 for diagonal disorder and in α_2 in case of off-diagonal disorder. Ignoring such contributions will make all moments greater than or equal to eight to be nonexact for diagonal and three for off-diagonal disorder. The ICPA achieves accuracy through self-consistency in the subspace of single fluctuations in it's present version, while the ASR achieves accuracy by increasing the number of recursions in the *full* augmented space and estimating the terminator to mimic the asymptotic part of the continued fraction as closely as possible. The two are very different algorithms. Both can take care of off-diagonal disorder and short-ranged order, but in those situations where clustering, either chemical or statistical, is important, the ASR, which takes into account correlated scattering from clusters, should be preferable over the single-fluctuation only version of the ICPA.

IV. FIRST-PRINCIPLES CALCULATIONS OF FORCE CONSTANTS IN ALLOYS

As is clear from the above discussions that the crucial component in both the ASR and the ICPA is the alloy force constants. Due to the random chemical environment around each atom in a substitutionally disordered alloy, the force constants corresponding to *A*-*A*, *B*-*B*, and *A*-*B*, pairs in a A_xB_{1-x} alloy are different and in no way resembles the force constants in a completely ordered environment. In order to have significant accuracy in calculated phonon properties one should, therefore, have accurate information on force constants corresponding to various pairs of chemical species. The only trustworthy source of force constant data is the first-principles calculation. To this end, we have employed first-principles density functional perturbation theory (DFPT) to obtain force constants. The details about the DFPT and our approach to use it to extract random alloy force constants is discussed below.

A. Density functional perturbation theory

Density functional perturbation theory (DFPT)[1] is a density functional theory (DFT) based linear response method to obtain the electronic and lattice dynamical properties in condensed matter systems. The dynamical matrix which provides information on lattice dynamics of the system can be obtained from the ground-state electron charge density and it's linear response to a distortion of the nuclear geometry.[34] In DFPT, this linear response is obtained within the framework of DFT. One of the greatest advantages of DFPT—as compared to other nonperturbative methods for calculating lattice dynamical properties of crystalline solids (such as the frozen-phonon or molecular dynamics spectral analysis methods)—is that within DFPT the responses to perturbations of different wave lengths are decoupled. This feature

TABLE I. Real-space nearest-neighbor force constants for $Fe_{50}Pd_{50}$ obtained by DFPT calculations on the artificial ordered structure. The units are dyn cm^{-1}.

Pair	Force constant	Direction
Fe-Fe	−9458	1*xx*
Fe-Pd	−9458	1*xx*
Pd-Pd	−28 974	1*xx*
Fe-Fe	−6005	1*xy*
Fe-Pd	−10 755	1*xy*
Pd-Pd	−30 372	1*xy*
Fe-Fe	1800	1*zz*
Fe-Pd	−114	1*zz*
Pd-Pd	3555	1*zz*

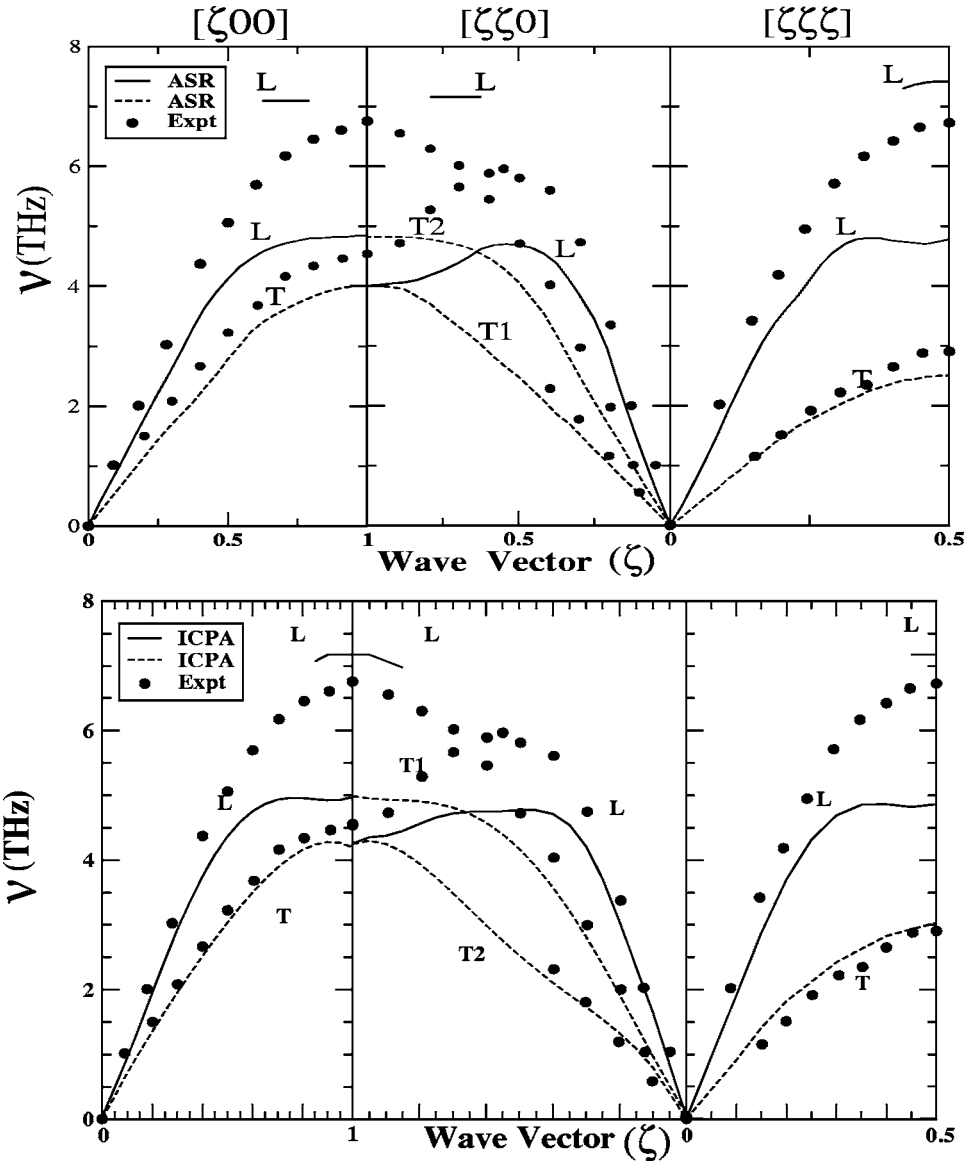

FIG. 1. Dispersion curves (frequency ν vs reduced wave vector ζ) for $Fe_{50}Pd_{50}$ alloy. The upper panel corresponds to the ASR results however the lower panel to the ICPA results. The filled circles are the experimental data (Ref. 41). The force constants used are given in Table I.

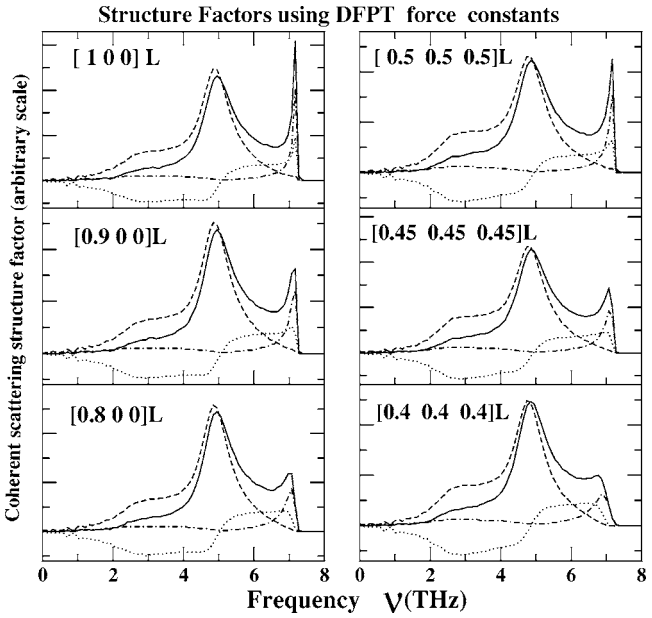

FIG. 2. Partial and total structure factors calculated in the ICPA for various ζ values along the $[\zeta,0,0]$ and $[\zeta,\zeta,\zeta]$ directions in $Fe_{50}Pd_{50}$ alloy. The type of mode is labeled along a particular symmetry direction. The force constants used are given in Table I. The solid curves, the dashed curves, the dotted-dashed curves and the dotted curves represent the total, the Fe-Fe, the Pd-Pd, and the Fe-Pd contributions, respectively.

allows one to calculate phonon frequencies at arbitrary wave vectors avoiding the use of supercells and with a workload that is independent of the phonon wavelength.

B. Random alloy force constants from density functional perturbation theory

Since there is no first-principles theory for lattice dynamics in random alloys available we took recourse to calculate force constants for ordered structures which can suitably mimic the random alloy using DFPT. However, for a proper representation for the random alloy, one needs to work with a large supercell which prohibits the use of DFPT from a practical point of view. The other approach would have been to construct a set of ordered structures having the same composition of the alloy under investigation, run first-principles calculation on each of them and average the data appropriately. As a first approximation to this approach, here we have done DFPT calculations on a single ordered structure and used the resultant force constants as approximate random alloy force constants as inputs to the ICPA and the ASR. The alloy chosen is FePd. The reason for choosing the FePd system is twofold: first, the ICPA and the ASR were applied only for the NiPt and NiPd alloys where the constituents of the alloys have face-centered-cubic structure in their elemental phases. In case of FePd, although the alloy in the disordered phase is face-centered cubic but Fe is body-centered cubic in it's elemental phase. It was therefore interesting to test the suitability of both the approximations in case of such a system where one of the constituents forming the alloy has a different structure than the alloy itself in it's elemental phase. Second, inelastic neutron scattering data were available for $Fe_{50}Pd_{50}$.[41] It would therefore have been possible to compare the ICPA and the ASR results with the experimental data directly enabling the understanding of the nature of interactions between various pairs of species in the random phase. Since the $Fe_{50}Pd_{50}$ forms a face-centered-cubic (fcc) solid solution, we have chosen the prototype tetragonal $L1_0$ structure with c/a ratio equal to unity to be used for first-principles calculations.

C. Details of first-principles calculations

We use DFPT within the local-density approximation (LDA) to compute the force constants for the FePd equiatomic composition single ordered structure mentioned above. The experimental lattice constant $a=7.24$ a.u. is used in the calculations. We employ a plane-wave pseudopotential implementation of the DFPT with Perdew-Zunger parametrization of the LDA[35] as done in the quantum-espresso package.[36] Ultrasoft pseudopotentials[37] with nonlinear core correction[38] are used for Fe and Pd. The kinetic energy cutoff is taken to be 35 Ry. The Brillouin-zone integrations are carried out with Methfessel-Paxton smearing[39] using a $10\times7\times7\times\mathbf{k}$-point mesh, which corresponds to 120 $\mathbf{k}$-points in the irreducible wedge. The value of the smearing parameter is 0.1 Ry. These parameters are found to yield phonon frequencies converged to within 5 cm^{-1}.

Once adequate convergence is achieved for the electronic structure, the phonon force constants are obtained using the linear response. Within DFPT, the force constants are conveniently computed in reciprocal space on a finite $\mathbf{q}$-point grid and Fourier transformation is employed to obtain the real-space force constants. The number of unique real-space force constants and their accuracy depend upon the density of the $\mathbf{q}$-point grids: the closer the $\mathbf{q}$-points are spaced, the more accurate the force constants are. In this work, the dynamical matrix is computed on a $6\times6\times4$ $\mathbf{q}$-point mesh[40] commensurate with the $\mathbf{k}$-point mesh.

V. RESULTS AND DISCUSSIONS

In Table I we report the nearest-neighbor force constants for the artificial ordered structure A-B obtained from first principles as described above. Subsequently, we use these force constants as inputs to the ICPA and the ASR calculations. Figure 1 shows the corresponding dispersion curves. The results clearly show that the force constants for the artificial ordered structure are not adequate to describe the lattice dynamics for the disordered $Fe_{50}Pd_{50}$ system. In both the ICPA and the ASR, the high frequency phonons are poorly represented for all three symmetry directions. On top of that, the high frequency branches suffer a split for large q values, a feature not observed in the experiments. All these features point to the fact that the first-principles force constants used in the ICPA and the ASR calculations fail to capture the complexities of the force-constant disorder in a random environment. This is quite understandable as we have used a crude approximation for the force constants in random environment. One single ordered structure, in no way, can

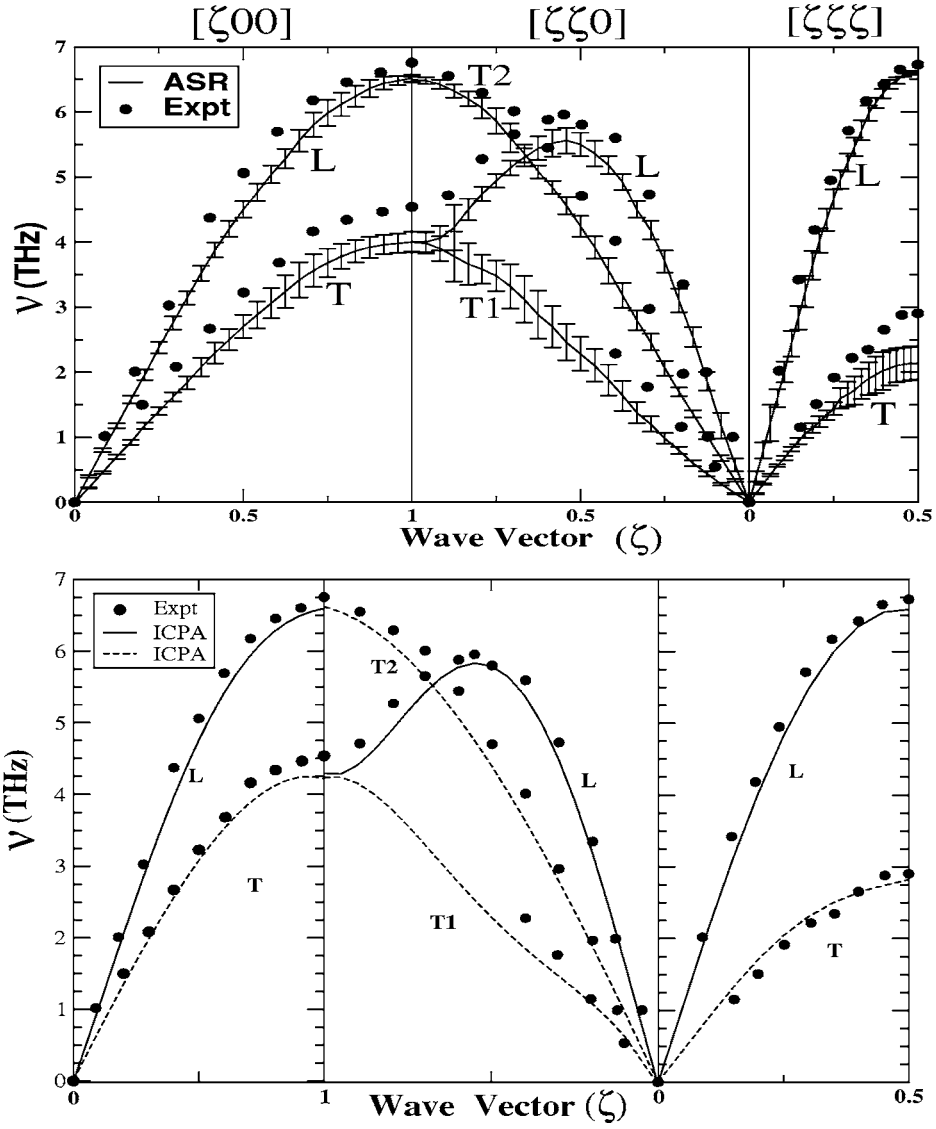

FIG. 3. Dispersion curves (frequency ν vs reduced wave vector ζ) for $Fe_{50}Pd_{50}$ alloy. The upper panel corresponds to the ASR results however the lower panel to the ICPA results. The filled circles are the experimental data (Ref. 41). The error bar in the ASR result basically represents the full widths at half-maxima (FWHM) at various ζ values. The force constants used are given in Table II.

mimic the randomness in the environment around a given chemical species. The fact that the force constants obtained on this artificial structure are responsible for the disagreement with the experiment is corroborated by the coherent structure factors, particularly at high q values as demonstrated in Fig. 2 where coherent structure factors for certain high q values, obtained by the ICPA, are displayed. The curves clearly show that the spurious high frequency peak is due to the Pd-Pd pairs and to a smaller extent due to Fe-Pd pairs. As is seen from Table I, the Fe-Fe and Pd-Pd force constants differ by about 70%, thereby representing a situation of very strong disorder as is seen in the case of $Ni_{50}Pt_{50}$.[3] The splitting of the high frequency branch is a manifestation of this strong force-constant disorder, albeit wrong in the present case.

In the pursuit of a quantitatively better set of force constants for the system so, that the suitability of the ICPA and the ASR can be properly tested, we went ahead and used the force constant data as reported in experiments.[41] The force constant data were obtained by fitting a Born–Von-Karman force constant model to the frequencies were obtained from neutron-scattering data on the ordered L10 FePd at 860 K, very close to the order-disorder transition temperature 950 K. The reason behind using the experimental force constants obtained from an ordered $L10$ structure for disordered calculations were twofold: first, the $L10$ force constants should be a better approximation for random alloy force constants than the artificial cubic structure ones because the $L10$ structure allows structural relaxation and therefore a variation in the bond distances between different chemical species pairs although in a restricted way. Nevertheless, this restricted degree of relaxation could be crucial in capturing the nature of forces between various chemical species as has been seen in the case of NiPt alloys.[42] Second, since the $L10$ data was taken at 860 K and the disordered fcc data was taken at 1020 K, both of them lie very close to the order-disorder transition temperature. At a first-order order-disorder transformation at finite temperatures, the ordered phase is only partially ordered and the disordered phase, it is in equilibrium with, has short-range order. Examination of the correlation functions has shown that ordered and disordered states rather show similar atomic arrangement in the vicinity of the order-disorder transformation. It is therefore expected that in the present case, the $L10$ force constants at

TABLE II. Real-space nearest-neighbor force constants for $Fe_{50}Pd_{50}$ obtained from experimental data (Ref. 41) on $L1_0$ structure at 860 K. The units are dyn cm^{-1}.

Pair	Force constant	Direction
Fe-Fe	−5650	1*xx*
Fe-Pd	−14050	1*xx*
Pd-Pd	−19 450	1*xx*
Fe-Fe	−9750	1*xy*
Fe-Pd	−16 550	1*xy*
Pd-Pd	−22 350	1*xy*
Fe-Fe	4100	1*zz*
Fe-Pd	2500	1*zz*
Pd-Pd	2900	1*zz*

860 K would not change significantly in the disordered phase at 1020 K. These intuitive arguments are well supported by the dispersion curves presented in Fig. 3. Both the ICPA and the ASR results agree reasonably well with the experimental data. The spurious splitting obtained earlier disappears. This disappearance can be understood better if we look at the force constants used for this calculation. Table II lists the experimental force constants used as inputs for the ICPA and the ASR calculations.

In comparison with DFPT values, the Pd-Pd force constants are a lot softer and the Fe-Pd force constants harden. The fact that the force constants and their behavior is indeed the deciding factor is again exemplified by the coherent structure factors for the selected high q vectors as shown in Fig. 4. The figures show that the single high frequency peak is now mostly because of the Fe-Fe and Fe-Pd contributions, rather than the Pd-Pd contribution. This points to the fact that the Pd-Pd contribution was overestimated and the Fe-Fe and the Fe-Pd contributions were grossly underestimated by the DFPT calculations on the artificial cubic structure because of the lack of relaxation in such structure. This in turn can be understood by looking at the bond distances between various pairs of species. In the cubic structure, the Fe-Fe, Pd-Pd, and the Fe-Pd distances were the same and in the present case was taken to be 5.12 a.u. The $L1_0$ structure at 860 K, on the other hand, had Fe-Fe and Pd-Pd distances to be 5.25 a.u. and the Fe-Pd distances to be 5.08 a.u. Thus, the Pd atoms, in the artificial cubic structures, were made to vibrate in a smaller volume and because of the smaller distance between two like atoms, the Pd-Pd force constants became harder. Figure 5 compares the ICPA and the ASR results for the phonon densities of states. Both the approximations produce identical features. The peaks and the band edges have quantitative agreement among themselves and with the experimental results.[41]

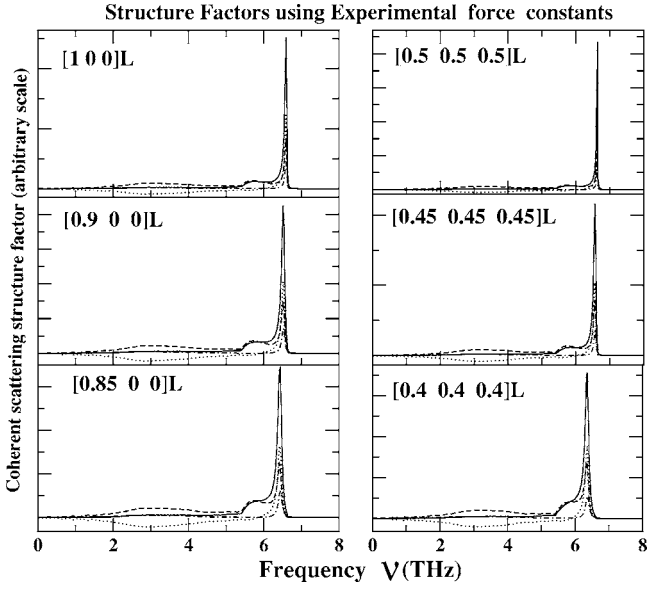

FIG. 4. Partial and total structure factors calculated in the ICPA for various ζ values along the $[\zeta,0,0]$ and $[\zeta,\zeta,\zeta]$ directions in $Fe_{50}Pd_{50}$ alloy. The type of mode is labelled along a particular symmetry direction. The force constants used are given in Table II. The solid curves, the dashed curves, the dotted-dashed curves, and the dotted curves represent the total, the Fe-Fe, the Pd-Pd, and the Fe-Pd contributions, respectively.

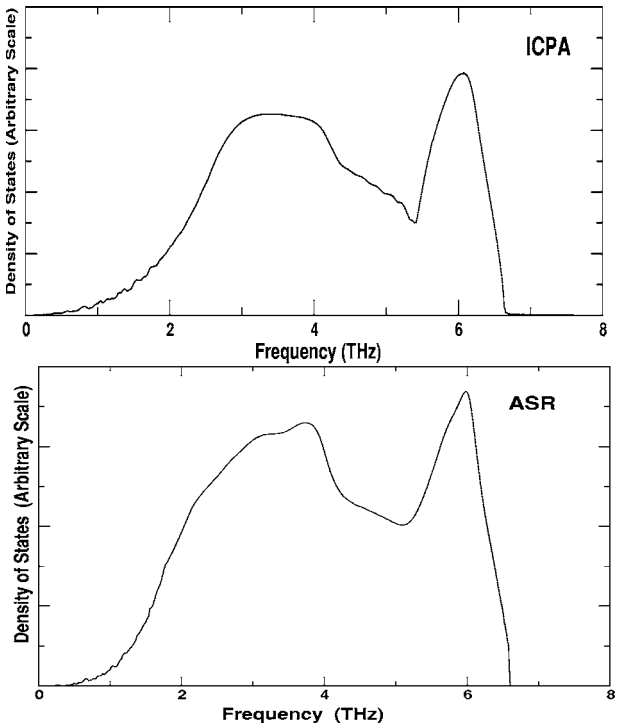

FIG. 5. Phonon density of states for $Fe_{50}Pd_{50}$ alloy. The upper and lower panels show the ICPA and ASR results, respectively. The force constants used are that of the experimental paper (Ref. 41) given in Table II.

Figure 6 displays the full width at half-maxima (FWHM) data associated with the finite lifetimes of phonons due to disordered scattering. The upper three panels show the widths as a function of wave vector (ζ) along the three symmetry directions extracted from the ASR method, while the lower three panels show the ICPA results. There are some quantitative differences between the two results. This is to be expected because the FWHM is extremely sensitive to the

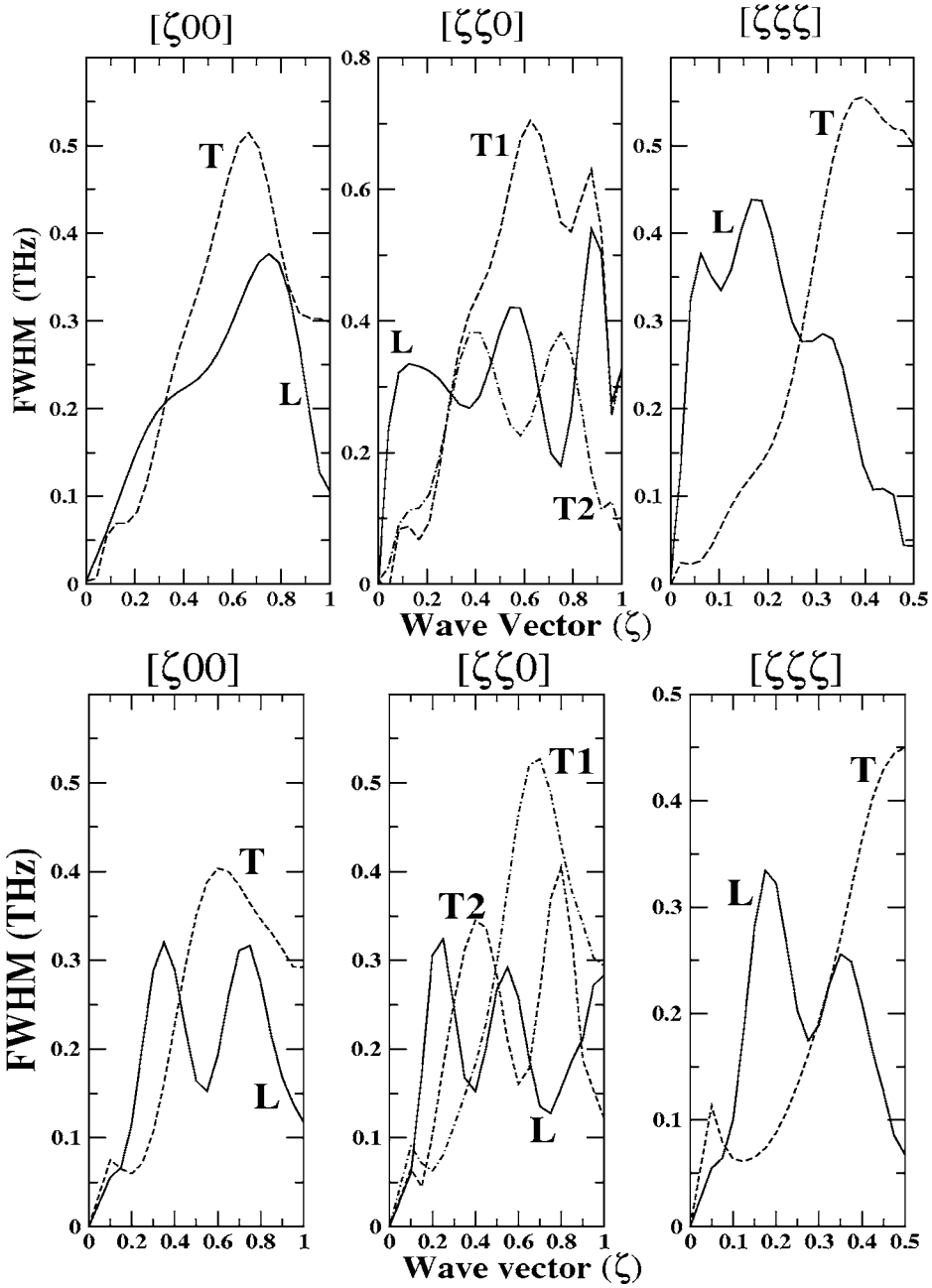

FIG. 6. Disorder-induced FWHM's vs wave vector (ζ) for $Fe_{50}Pd_{50}$ alloy. The upper and lower panels show ASR and ICPA results, respectively. The force constants used are given in Table II.

underlying approximation. However, a careful look suggestes that the important peaks and valleys occur nearly at the same positions. At this point we are unable to comment upon which approximation fares better because of the unvailability of experimental data.

In Fig. 7, we have shown the total coherent structure factors at various ζ values along the three symmetry directions with various modes of vibrations. The upper box shows the ASR result while the lower shows the ICPA result. In both the cases, the different curves for different ζ values are shifted along the x axis in order to facilitate vision. At a first glance it may appear that the two results are rather different. However, a careful look will convince us that the apparent difference arises because of the different ways in which the coherent structure factors are calculated by the ICPA and ASR. In the ICPA the structure factors are separately calculated for each branch, transverse and longitudinal, along each symmetry direction. That is why the ICPA shows seven panels. In the ASR, on the other hand, the L and T branches for $[\zeta\zeta 0]$ and $[\zeta\zeta\zeta]$ directions are calculated together. These panels show two peaked structures. A careful inspection shows that the peak positions are almost identical in the two methods. The almost similar dispersion curves of Fig. 3 is a testimony to this statement.

Another important point of this figure are the qualitative similarities in the line shapes in the two approximations. They are generally sharp peaked for low wave vectors, wider but symmetrical for the medium wave vectors and wide and asymmetric for large wave vectors for all the three symmetry directions for both ICPA and ASR. The structure factors from ICPA and ASR are quite close as far as peak positions and shapes are concerned.

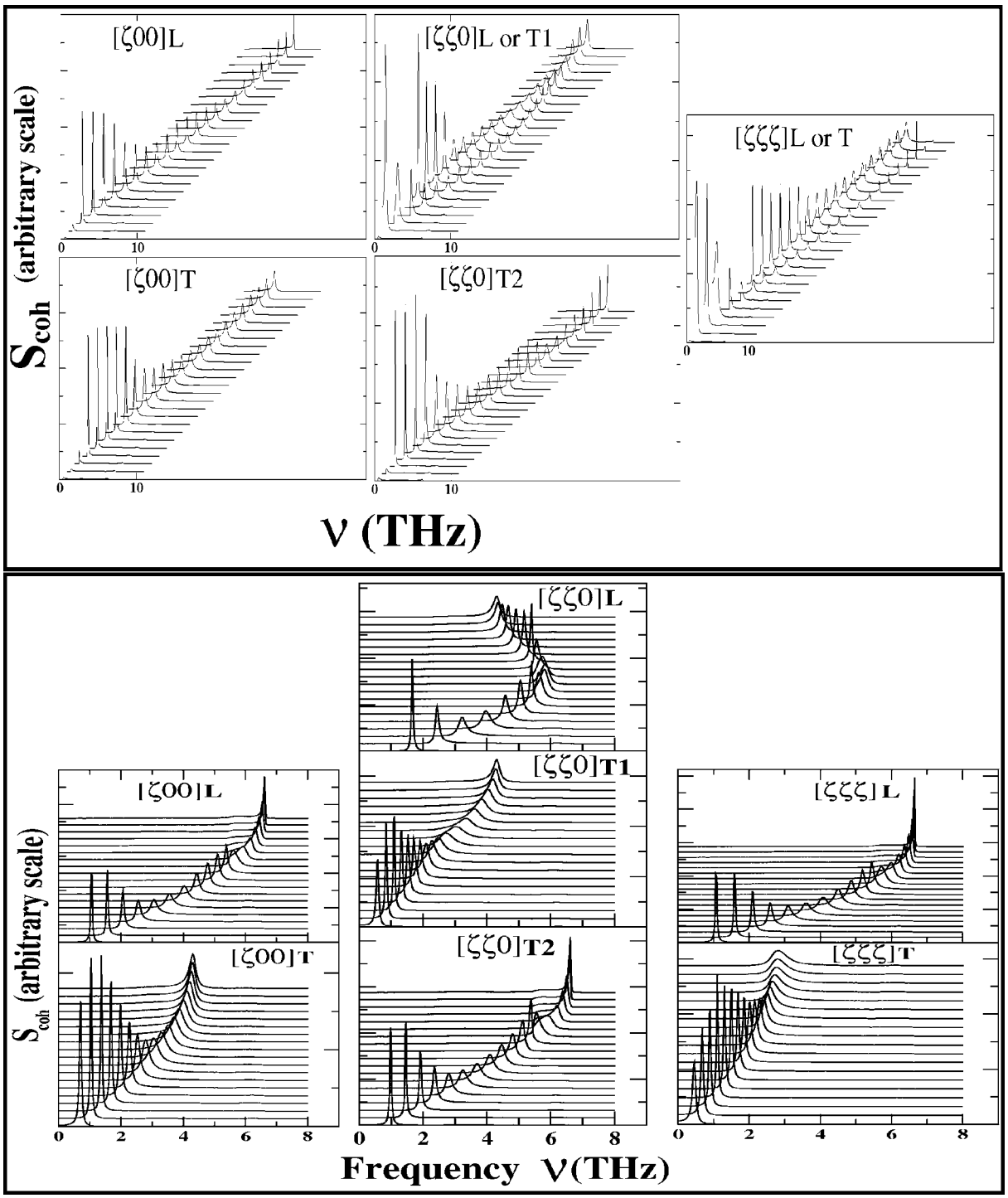

FIG. 7. Total coherent structure factors in different directions with different branches for $Fe_{50}Pd_{50}$ alloy. The upper and lower box shows ASR and ICPA results, respectively. In each of the different directions and branches, the various curves indicate the total structure factors for various ζ values starting from the lowest value to the edge of the Brillouin zone. In both the boxes, the different curves for different ζ values are shifted along the x axis in order to facilitate vision.

VI. CONCLUSIONS

This paper has continued the development of the augmented-space recursion[2] and the itinerant coherent potential approximation (ICPA)[3] for studying the vibrational properties of disordered metallic alloys. A brief description of the two methods combined with a first-principles calculation (the so-called DFPT) of the dynamical matrices has been reported. The power of these approaches has been illustrated by explicit calculations on the $Fe_{50}Pd_{50}$ alloy.

Both the theories are unique and systematic in the sense that they produce almost identical results for a particular system. Both the theories can explicitly take into account the

fluctuations in masses, force constants and scattering lengths. We propose the methods as computationally fast and accurate techniques for the study of lattice dynamics of disordered alloys. A correct quantitative trend (comparable to the experimental results) of the phonon dispersion and the phonon density of states has been predicted by both the methodologies when the experimental force constants has been used in the calculation. Of course there is a fairly obvious general comment to be made with regard to the self-consistency of the procedure. This is precisely the reason that a first-principles estimate of the dynamical matrices on parent ordered alloys do not yield quantitatively accurate results (in comparison with the experiment) for the disordered alloy. We shall propose that we need to go beyond and estimate the dynamical matrices from a model of embedded atoms in a fully disordered background.

ACKNOWLEDGMENT

One of the authors (A.A.) would like to acknowledge the CSIR for financial assistance in the form of a grant.

*On sabbatical leave from: S.N. Bose National Centre for Basic Sciences, Kolkata, India.

[1] S. Baroni, S. De Gironcoli, A. Dal Corso, and P. Giannozzi, Rev. Mod. Phys. **73**, 515 (2001).

[2] A Alam and A Mookerjee, Phys. Rev. B **69**, 024205 (2004).

[3] S. Ghosh, P. L. Leath, and M. H. Cohen, Phys. Rev. B **66**, 214206 (2002).

[4] D. W. Taylor, Phys. Rev. **156**, 1017 (1967).

[5] A complex function $f(z)$ is called *herglotz* if (i) all its singularities lie on the real z axis (ii) $\mathrm{Im}\, f(z)$ is negative everywhere in the plane $\mathrm{Im}(z)>0$ and is positive everywhere in $\mathrm{Im}(z)<0$ (iii) $\lim_{z=E\to\pm\infty} \mathrm{Re}\, f(E)=0$, E is real.

[6] E. Müller-Hartmann, Solid State Commun. **12**, 1269 (1973).

[7] N. Kunimoto, Y. Tsunoda, and Y. Hirai, Solid State Commun. **13**, 495 (1973).

[8] T. Kaplan and M. Mostoller, Phys. Rev. B **9**, 353 (1974).

[9] W. A. Kamitakahara, Bull. Am. Phys. Soc. **19**, 321 (1974).

[10] W. A. Kamitakahara and D. W. Taylor, Phys. Rev. B **10**, 1190 (1974).

[11] M. Mostoller, T. Kaplan, N. Wakabayashi, and R. M. Nicklow, Phys. Rev. B **10**, 3144 (1974).

[12] H. G. Smith and N. Wakabayashi, Bull. Am. Phys. Soc. **21**, 410 (1976).

[13] T. Saha, I. Dasgupta, and A. Mookerjee, J. Phys.: Condens. Matter **8**, 1979 (1996).

[14] A. Mookerjee and R. Prasad, Phys. Rev. B **48**, 17724 (1993).

[15] D. Paudyal, T. Saha-Dasgupta, and A. Mookerjee, J. Phys.: Condens. Matter **16**, 2317 (2004).

[16] H. Shiba, Prog. Theor. Phys. **40**, 942 (1968).

[17] T. Kaplan and M. Mostoller, Phys. Rev. B **9**, 353 (1974).

[18] B. Nickel and W. H. Butler, Phys. Rev. Lett. **30**, 373 (1973).

[19] F. Ducastelle, J. Phys. C **7**, 1795 (1974).

[20] A. Gonis and J. W. Garland, Phys. Rev. B **18**, 3999 (1978).

[21] A. Mookerjee, J. Phys. C **6**, 1340 (1973).

[22] T. Saha, I. Dasgupta, and A. Mookerjee, Phys. Rev. B **50**, 13267 (1994).

[23] R. Mills and P. Ratanavararaksa, Phys. Rev. B **18**, 5291 (1978).

[24] T. Kaplan, P. L. Leath, L. J. Gray, and H. W. Diehl, Phys. Rev. B **21**, 4230 (1980).

[25] R. Haydock, V. Heine, and M. J. Kelly, J. Phys. C **5**, 2845 (1972).

[26] D. A. Rowlands, J. B. Staunton, B. L. Gyorffy, E. Bruno, and B. Ginatempo, Phys. Rev. B **72**, 045101 (2005).

[27] D. A. Biava, S. Ghosh, D. D. Johnson, W. A. Shelton, and A. V. Smirnov, Phys. Rev. B **72**, 113105 (2005).

[28] M. Jarrell and H. R. Krishnamurthy, Phys. Rev. B **63**, 125102 (2001).

[29] A. Mookerjee, in *Electronic Structure of Alloys, Surfaces and Clusters*, edited by A. Mookerjee and D. D. Sarma (Taylor Francis, London, 2003).

[30] V. Kumar, A. Mookerjee, and V. K. Srivastava, J. Phys. C **15**, 1939 (1982).

[31] S. Ghosh, N. Das, and A. Mookerjee, Int. J. Mod. Phys. B **21**, 723 (1999).

[32] R. Haydock, *Solid State Physics* (Academic Press, New York, 1980), Vol. 35.

[33] N. Beer and D. G. Pettifor, in *Electronic Structure of Complex Systems*, edited by P. Phariseau and W. M. Tammerman (Plenum, New York, 1984), p. 769.

[34] R. Pick, M. H. Cohen, and R. M. Martin, Phys. Rev. B **1**, 910 (1970); P. D. De Cicco and F. A. Johnson, Proc. R. Soc. London, Ser. A **310**, 111 (1969).

[35] J. P. Perdew and A. Zunger, Phys. Rev. B **23**, 5048 (1981).

[36] S. Baroni, A. Dal Corso, S. de Gironcoli, and P. Giannozzi, http://www.Quantum-Espresso.org

[37] D. Vanderbilt, Phys. Rev. B **41**, 7892 (1990).

[38] S. G. Louie, S. Froyen, and M. L. Cohen, Phys. Rev. B **26**, 1738 (1982).

[39] M. Methfessel and A. T. Paxton, Phys. Rev. B **40**, 3616 (1989).

[40] P. Giannozzi, S. de Gironcoli, P. Pavone, and S. Baroni, Phys. Rev. B **43**, 7231 (1991).

[41] T. Mehaddene, E. Kentzinger, B. Hennion, K. Tanaka, H. Numakura, A. Marty, V. Parasote, M. C. Cadeville, M. Zemirli, and V. Pierron-Bohnes, Phys. Rev. B **69**, 024304 (2004).

[42] S. Ghosh, J. B. Neaton, A. H. Antons, M. H. Cohen, and P. L. Leath, Phys. Rev. B **70**, 024206 (2004).